JOURNAL OF MATERIALS SCIENCE 32 (1997) 5497–5503

Microstructures and mechanical properties of mullite–(yttria, magnesia- and ceria-stabilized) zirconia composites

THAN MIN KYAW, Y. OKAMOTO*, K. HAYASHI
Department of Chemistry and Materials Technology, Kyoto Institute of Technology, Matsugasaki, Sakyo-ku, Kyoto 606 Japan

The microstructures and some mechanical properties of composites containing mullite and each of three different zirconias stabilized with low concentrations of yttria, magnesia, and ceria, have been studied. A sol–gel derived, high-purity, mullite was used as a matrix phase. In the present study, composites were prepared by conventional sintering of mullite and zirconia milled powder mixture. In all the composite materials, large fractions of the tetragonal zirconia (ZrO_2) transformed into monoclinic form during cooling from the fabrication temperature. In the use of ceria-stabilized ZrO_2, large internal macroscopic voids appeared in the sintered body. The thermal expansion hysteresis associated with the tetragonal/monoclinic transformation was evident only in the mullite/yttria-stabilized ZrO_2 composite from which the M_s temperature could be determined.

1. Introduction

High melting point, low thermal expansion coefficient, chemical inertness, thermal stability (good thermal shock resistance), excellent high-temperature strength and creep resistance are technically attractive properties of mullite for potential high-temperature structural applications [1–8]. Several methods for fabricating mullite powders using advanced powder technologies have been developed, (see Ref. [9]), among which a sol–gel method is commonly known to produce pure and fine mullite powders. A dense polycrystalline mullite with stoichiometric composition $3Al_2O_3 \cdot 2SiO_2$ obtained by sintering the sol–gel derived mullite powders at 1650 °C [10] gives a flexural strength of 450 MPa and a toughness of 2.73 MN $m^{-1.5}$.

Meanwhile, tetragonal ZrO_2 polycrystals (TZP) partially stabilized with oxides such as Y_2O_3, CeO_2, and MgO have been found to be relatively stronger and tougher ceramic materials, due to the occurrence of stress-induced martensitic phase transformation of the stabilized t-ZrO_2 in the propagating crack tip [11–14]. Toughness values of 6–9 MN $m^{-1.5}$ with a flexural strength of about 700 MPa can be achieved in the t-ZrO_2 polycrystals stabilized with low concentrations of yttria [11] (Y–TZP). Hence, the dispersion of ZrO_2 particles in mullite has been devoted to enhancing the room-temperature fracture toughness and strength [15–18].

Three different zirconias stabilized with 2 mol % yttria, 9 mol % magnesia, and 12 mol % ceria (denoted 2Y–TZP, 9Mg–PSZ, and 12Ce–TZP, respectively) were chosen for the present study because their equilibrium phase diagrams of the ZrO_2-rich portion show a wide range of tetragonal (t) solid-solution region [19–21]. Grain size, in addition to the concentration of stabilizer, is a factor controlling the stability of tetragonal phase. Becher and Swain [22] have pointed out that the metastable tetragonal phase can fully be retained in the 12Ce–TZP with grain sizes up to 8 μm or greater, while those of < 1 μm are required for the 2Y–TZP. In the case of MgO-partially stabilized zirconia, sintering at temperatures about 1750 °C is necessary (for a cubic solid-solution region) with a controlled cooling, during which t-ZrO_2 precipitates form and grow within the cubic ZrO_2 matrix. A "subeutectoid" ageing [23] at about 1100 °C is often conducted to enhance the transformability of the t-ZrO_2 precipitates, which significantly improves the mechanical properties. Microstructure and properties of mullite–zirconia composites prepared by various methods, such as coprecipitation and the sol–gel method, and the reaction *in situ* method, have been investigated by many workers [16, 24–27]. In the present work, mullite–ZrO_2 composites were fabricated by means of a powder mixing and sintering method.

2. Experimental procedure

Sol–gel derived, fine-grained mullite powder (MP-40, Chichibu Cement Co.) and zirconia powders partially stabilized by yttria and magnesia (2Y–TZP and 0Z–9Mg, Osaka Cement Co.), and ceria (TZ–12Ce,

* Author to whom all correspondence should be addressed.

0022–2461

Tosoh Corp.) were used as starting materials. The appropriate amounts of mullite and 15 vol % of each ZrO_2 powder were mixed by a conventional ball milling using zirconia balls in isopropanol for 24 h. The resulting paste obtained after milling was dried in a rotary-vacuum evaporator and in an oven, then, ground and sieved to produce agglomerate-free powders. Next, the powder mixtures were calcined at 800 °C for 1 h to flash off any volatile organic contamination, pressed uniaxially (15 MPa) and isostatically (200 MPa) prior to a subsequent sintering at 1610 °C for 3 h in air. Appropriate sintering temperatures for mullite and composites were 1630 and 1610 °C respectively [24], and those for 2Y–TZP and 12Ce–TZP were chosen at 1400 °C while 9Mg–PSZ was sintered at 1760 °C for 3 h followed by slow cooling and annealing at 1100 °C for 1 h. The crystalline phases present in the sintered billets were identified by X-ray diffractometry (CuK_α, Rigaku RV-200). The ZrO_2 phase was ascertained when existing in the metastable tetragonal (t) and in the monoclinic (m) form in regard to the Toraya's calibration method [28]. The sintered density was measured by immersion in water using Archimedes' principle on test bars (4 mm × 3 mm × 45 mm) which were first sawn from the sintered billets. Flexural strength was measured by four-point bending method (spans of 30 and 10 mm). Fracture toughness and hardness were measured on the polished surface by Vicker's indentation fracture method, in accordance with the Marshall and Evan's method [29]. Microstructures were characterized by SEM (S-800, Hitachi) and the average grain sizes were determined from the micrographs using the line intercept method. Thermal expansion measurements were conducted in the temperature range from room temperature to 900 °C at heating and cooling rate of 5 K min^{-1} by means of dilatometry (TMA 8140, Rigaku) using high-grade quartz glass as reference.

3. Results and discussion

Materials employed in this work are summarized in Table I. For comparison, very fine-grained mullite–15 vol % ZrO_2, designated MZ–15#, which was received from Chichibu Cement Co. and prepared by the sol–gel method containing no stabilizer, was also used in this work.

Their microstructures are shown in Fig. 1. Darker and lighter phases are mullite and ZrO_2 grains, respectively, and the latter have a spheroidal shape. The ZrO_2 grains tended to possess concave boundary segments, whereas the mullite grains tended to be convex with crystallographic facets. Most of the ZrO_2 grains are relatively isolated (intergranular) within the mullite. The MZ–15# material exhibits very fine microstructure in which the ZrO_2 grains reside at grain boundaries and also intragranularly within the mullite grains.

Fig. 2 illustrates typical XRD results for the sintered ZrO_2 polycrystals and composites, and the former shows only the metastable tetragonal phase. However, cubic phases incorporating the t-ZrO_2 precipitates exist in the 9Mg–PSZ. In the case of composites, both monoclinic and tetragonal phases are observed, regardless of the stabilizers present and the finer grain size. That is, some t-ZrO_2 grains have transformed into m-form during fabrication. The two strongest m-ZrO_2 peaks, (1 1 $\bar{1}$) and (1 1 1) appearing at $\sim 28.2^\circ$ and at $\sim 31.5^\circ$, respectively, become stronger and the tetragonal (1 1 1) peak appearing at $\sim 30.2^\circ$, is negligible in the MZ–15C.

Characteristics of the sintered mullite and composites are indicated in Table II. All zirconia polycrystals give near theoretical density after sintering at 1400 °C for 2 h, and their averaged linear thermal expansion coefficient is about 11.5×10^{-6} K^{-1}; greater by about twice than that of mullite. Sintering temperatures of 1630 °C and above are generally required to obtain a highly dense mullite. The effect of ZrO_2 addition on densification (sinterability) of mullite is seen in the MZ–15Y and MZ–15# materials while the remainders, MZ–15M and MZ–15C are less dense bodies; large internal voids developed in the sintered MZ–15C body during fabrication (see Fig. 3). Over 50 vol % of the ZrO_2 grains exist in the m-form and the less dense bodies exhibit greater m-fractions. The greater m-fraction found in the MZ–15# is due to the absence of stabilizer, and as such, the 30 vol % retained t-ZrO_2 phase is, possibly, the result of its finer grain size. The stress-induced martensitic phase transformation of the retained t-ZrO_2 which occurred at a crack-tip field during fracturing caused the increment in m-ZrO_2 fractions on fracture surfaces. The mechanical stiffness of the matrix phase is considerable and the ZrO_2 grains in the dense body are subjected to a larger strain energy (i.e. constraint of the mullite matrix) compared with those in the less dense body so that the large strain energy would ensue if the t-to-m phase transformation occurs [30, 31], and thus the t-ZrO_2 grain in a porous body readily transforms to the less dense m-form, and that constrained by a matrix is stable in the t-phase.

The stability of the t-ZrO_2 phase is, in general, controlled by its grain size and the ZrO_2 grain growth is found in the composite, as seen from Table II, because it is subjected to sintering at the relatively higher

TABLE I Materials used in this study

Material	Ingredient	Stabilizer (mol %)
MZ–15Y	Mullite + 15 vol % ZrO_2 (2Y–TZP)	Y_2O_3, 2.0
MZ–15M	Mullite + 15 vol % ZrO_2 (9Mg–PSZ)	MgO, 9.0
MZ–15C	Mullite + 15 vol % ZrO_2 (12Ce–TZP)	CeO_2, 12.0
MZ–15#	Mullite + 15 vol % ZrO_2 (unstabilized)	

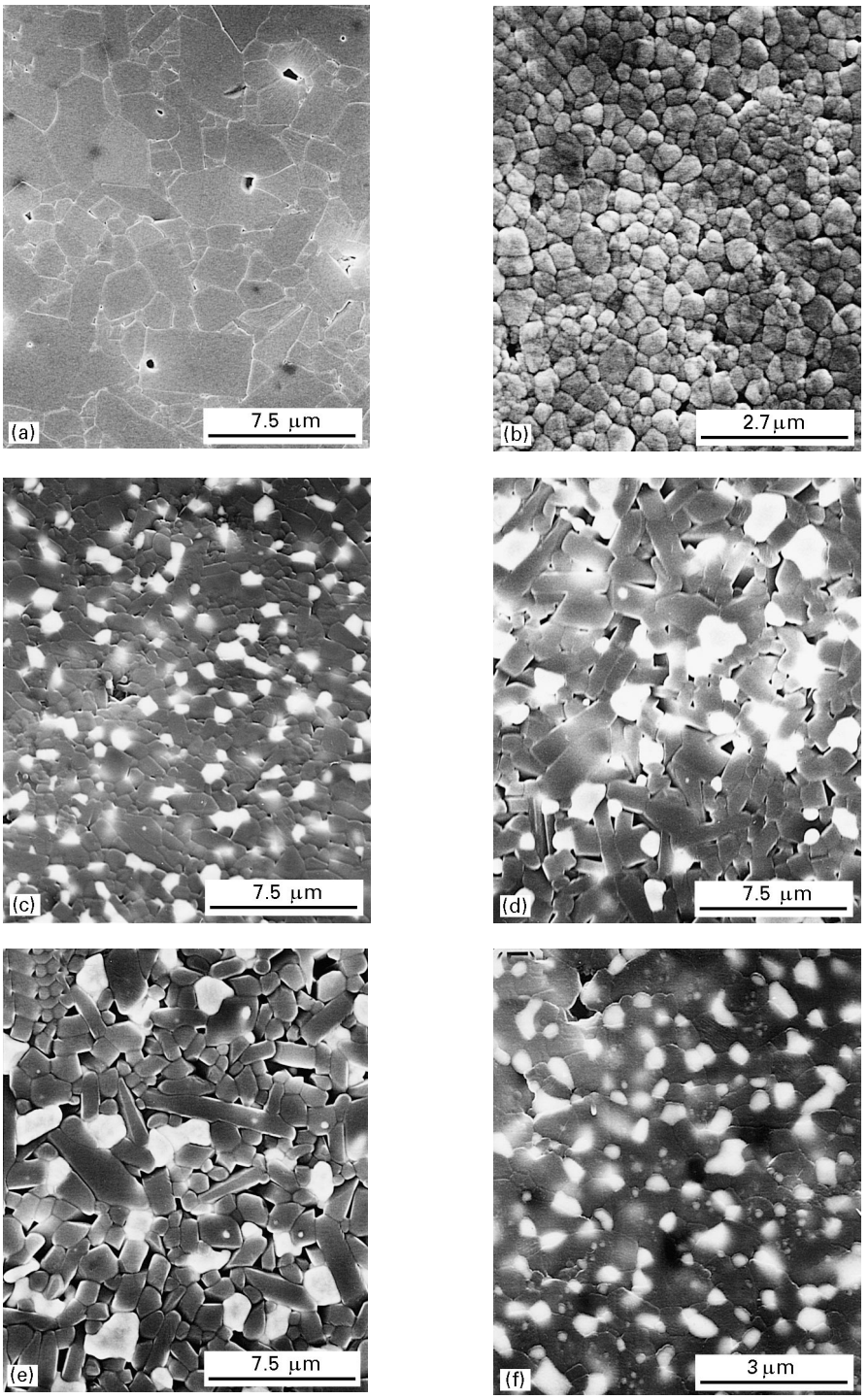

Figure 1 Microstructures of mullite, ZrO_2, and composites; (a) mullite, (b) ZrO_2 (2Y–TZP), (c) MZ–15Y, (d) MZ–15M, (e) MZ–15C, and (f) MZ–15#. Darker and lighter phases are mullite and ZrO_2 grains, respectively.

temperature. Tetragonal phase can be stable at ambient temperature even without any stabilizer if its particle size is finer than about 30 nm, i.e. the surface energy of the t-phase is smaller than that of the m-phase [13]. But instead, Mitsuhashi *et al.* [32] reported that grain growth provides active nucleation sites for phase transformation.

The possible reasons for the destabilization of the t-ZrO_2 phase in mullite matrix/ZrO_2 composite are not only the ZrO_2 grain size but also the internal stresses which develop in it during cooling, resulting from the thermal expansion mismatch between mullite and ZrO_2, as well as the content of stabilizer in solid solution in it. The large difference in thermal expansion coefficients between mullite matrix and ZrO_2 inclusions would introduce thermal stresses in the ZrO_2 grains during cooling from the sintering temperature. Because ZrO_2 has a higher thermal expansion coefficient, the t-ZrO_2 grains should be stressed in tension [33]. These internal tensile stresses are theoretically found to be 1.1 GPa by supposing them to be in an infinite matrix of mullite and contracting isostatically on cooling from 1610 °C to 500 °C [34]. Hence, the t-ZrO_2 grains, subjected to such high tensile stresses, undergo the t-to-m phase transformation at temperatures well below 1000 °C.

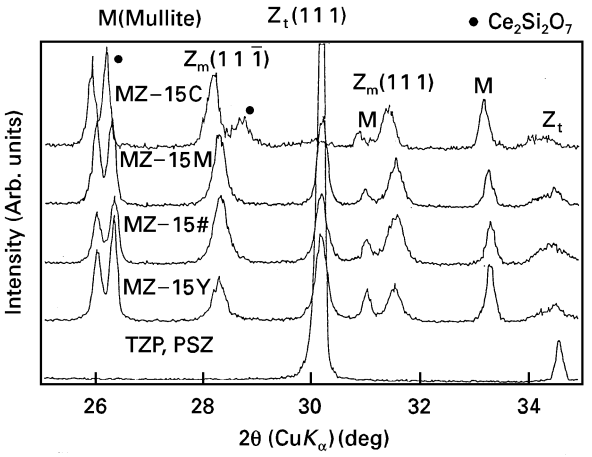

Figure 2 Typical XRD patterns of stabilized zirconia polycrystal (sintered at 1400 °C) and composites (sintered at 1610 °C). M, Z_m and Z_t denote mullite, monoclinic and tetragonal ZrO_2, respectively.

The stability of t-ZrO_2 phase relies also on the content of stabilizer in solid solution because the yttria stabilizer, for instance, has been known to possess a tendency to react with other oxides such as, in this work, Al_2O_3 and SiO_2 present in mullite at the sintering temperature, resulting in the t-ZrO_2 with a lack of yttria solid solution. The yttria stabilizer contained initially 2 mol % ZrO_2 and it is recognized that < 2 mol % ZrO_2 in solid solution cannot exist in the tetragonal phase unless its crystallite size is finer that 30 nm. The direct measurement of the concentration of yttria in zirconia could not, however, be readily done because its grain size is quite small. If some yttria reacts with alumina and/or silica from mullite during sintering, a second, oxide phase will be formed at the grain boundaries. So, we confirmed indirectly the presence of the glassy phase (of unknown chemical composition) which accumulates at the grain boundaries using a dilute hydrofluoric aqueous solution [35]. As a result, the t-ZrO_2 grains became deficient in yttria and the composition of ZrO_2–Y_2O_3 solid solution changed to a concentration range of yttria (< 2 mol %) where the stable phase at ambient temperature is monoclinic [19, 36]. Similarly, the enhanced phase transformation found in the use of Mg–PSZ and Ce–TZP, could be thought to be due to the formation of an unknown complicated compound resulting from the reaction between the stabilizer and mullite phase during sintering.

The presence of a grain-boundary glass phase, and the phase transformation behaviour of ZrO_2 in the MZ–15Y were described in detail elsewhere [35], but detailed studies on magnesia- and ceria-stabilized zirconia in mullite have not yet been performed.

TABLE II Characteristics of sintered mullite and composites

Material	Relative density (%)	m-ZrO_2 fraction		Grain size		Expansion coefficient[a], α (10^{-6} K^{-1})
		Sintered surface (vol %)	Fracture surface (vol %)	mullite (μm)	ZrO_2 (μm)	
Mullite	97.2	–	–	1.76	–	4.8
MZ–15Y	98.2	52	79	1.51	0.74	Temp. dependent
MZ–15M	96.0	67	88	1.70	1.22	5.4
MZ–15C	low	92	n.d.	1.69	1.26	n.d.
MZ–15#	98.5	70	92	0.88	0.29	5.2

[a] RT to 900 °C.

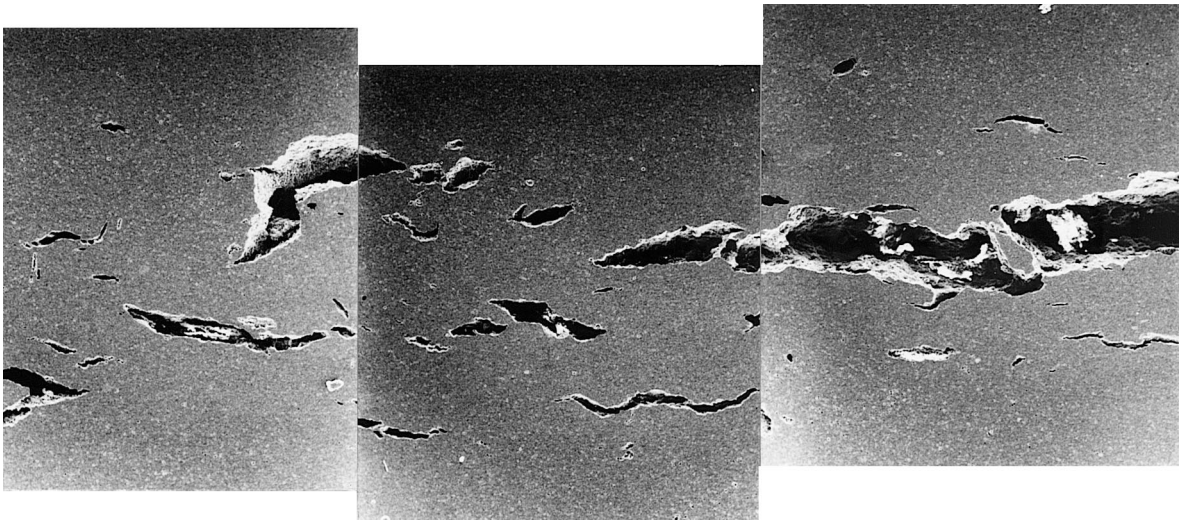

Figure 3 Scanning electron micrographs of cross-sectional surface of sintered MZ–15C composite illustrating longitudinal large internal voids. They also form vertically, resulting in surface bulging.

TABLE III Properties of materials described in Table II

Material	Hardness, H_V (GPa)	Toughness, K_{IC} (MN m$^{-1.5}$)	Strength, σ_f (MPa)	M_s temp.[a] (°C)
Mulite	11.6	2.13	314	–
MZ–15Y	12.8	2.96	347	613
MZ–15M	11.2	3.72	288	–
MZ–15C	n.d.	n.d.	n.d.	n.d.
MZ–15#	13.5	2.62	352	> 900
2Y–TZP	12.0	7.50	1086	< RT
9Mg–PSZ	–	11.50	599	< RT
12Ce–TZP	8.8	5.68	632	< RT

[a]M_s, Martensitic transformation start on cooling.

Some mechanical properties of the materials obtained are summarized in Table III. The effect of ZrO_2 incorporation in mullite on strengthening and toughening is found only in the MZ–15Y and MZ–15# materials, whereas the remainder (MZ–15M) resulted in strength degradation. The higher strength obtained in the MZ–15# material is due to the fine microstructure and, possibly, free of the glass phase. Properties of the MZ–15C material could not be determined because it contains large deleterious internal voids, which will be discussed later.

The presence of large m-ZrO_2 fractions in the surfaces of composites was thought to be responsible for the strength degradation because it has been recognized that the large volume increase and shear strains accompanied by the t-to-m phase transformation invariably cause microcracking [37]. On the contrary, the occurrence of phase transformation in the surface has been reported to be desirable in some cases, because residual surface compressions, resulting from the volume increase, improve strength [38–40]. Toughening may result from the microcrack deflection (known as microcrack toughening) or crack bowing, but the toughening mechanism in composites still remains unknown.

3.1. Mullite/12Ce–TZP composite (MZ–15C)

The addition of 12Ce–TZP into mullite causes a bulge on the surface of the composite body after sintering at 1610 °C in air which is not evident in the MZ–15Y, MZ–15M, and MZ–15# materials. This bulge develops due to the formation of large internal macroscopic voids, as shown in Fig. 3.

These large internal voids were formed possibly as a result of entrapped free oxygen gases which were believed to be produced from the reduction of Ce^{4+} (CeO_2) to a trivalent state, Ce^{3+} (Ce_2O_3). The following reaction expresses the reduction of CeO_2 to Ce_2O_3

$$2CeO_2 \rightarrow Ce_2O_3 \text{ (or } CeO_{1.5}) + 1/2\,O_2 \qquad (1)$$

CeO_2 undergoes the slight reduction or even sinters in air [41] and CeO_2/ZrO_2 solid solutions undergo more substantial reduction in air [42]. Many investigations pertaining to the phase relations in the zirconia–ceria systems at elevated temperature in air have been found [21, 43, 44]. Phase diagrams for the $CeO_{1.5}$–ZrO_2 and $CeO_{1.5}$–CeO_2–ZrO_2 (at 1400 °C) systems are described elsewhere [45]. The XRD result of MZ–15C composite (Fig. 2) shows $Ce_2Si_2O_7$ compound instead of the pyrochlore type compound (p-phase) with a composition of $Ce_2Zr_2O_7$ which is notified in the phase diagrams [45]. Thus, Ce_2O_3 tends to combine with SiO_2 present in the mullite during sintering, to form the $Ce_2Si_2O_7$ compound, prior to reoxidizing with the free oxygen gases to become Ce^{4+}(CeO_2) on cooling, according to Reaction 2

$$Ce_2O_3 + 2SiO_2 \rightarrow Ce_2Si_2O_7 \qquad (2)$$

$Ce_2Si_2O_7$ compound (which melts congruently at 1770 ± 25 °C) is generally formed by Reaction 2 at temperatures between 1350 and 1450 °C [46]. Therefore, destabilization of the t-ZrO_2 phase due to the lack of stabilizer in solid solution is also found in the MZ–15C composite. Solid solutions between Al_2O_3 and ZrO_2, and between Al_2O_3 and CeO_2 are not formed at temperatures < 1600 °C [47]. However, $CeAlO_3$ and $Ce_2O_3 \cdot 11Al_2O_3$ are reported to be stable at above 1600 °C in air and they decompose at 800 and 1200 °C, respectively, on cooling [48].

The diffusivity of the oxygen gas evolved from Reaction 1 through the bulk and out of the surface depends on many factors, such as temperature, lattice and boundary diffusion coefficients of the oxygen through neighbouring material (i.e. mullite), and a depth of the reduced Ce_2O_3 layer. Ando *et al.* [49] has reported oxygen (O^{2-}) self-diffusion coefficients in 14Ce–TZP (14 mol% ceria-stabilized ZrO_2) to be 2.3×10^{-8} cm^2 s^{-1} at 1400 °C, such that oxygen can diffuse only few hundreds of micrometers during the sintering process. Furthermore, the diffusivity of the oxygen ion is known to be smaller in mullite compared to that in the ZrO_2 phase. Therefore, if the depth of the Ce^{3+} layer is greater than the diffusible distance of the oxygen ion, the free oxygen gases will be entrapped in the mullite matrix phase on cooling, causing the surface to bulge.

3.2. Dilatation results

Because temperature-dependent, reversible tetragonal/monoclinic phase transformation is associated with volume expansion and contraction, dilatational measurement was carried out on the materials in the

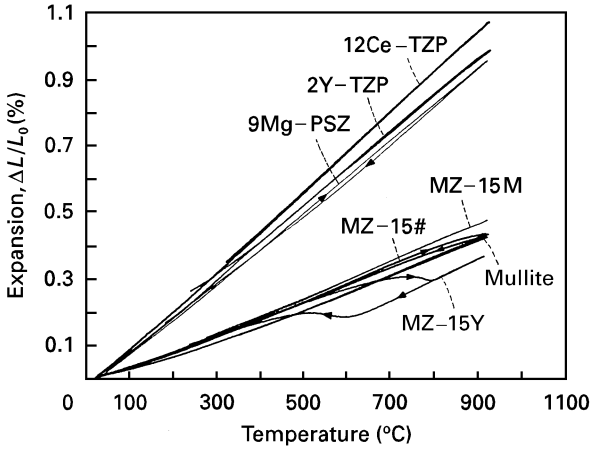

Figure 4 Thermal expansion curves of 12Ce–TZP, 2Y–TZP, 9Mg–PSZ, MZ–15M, MZ–15#, mullite, and MZ–15Y. Heating and cooling are indicated by arrows (heating and cooling rate = 5 °C min^{-1}).

temperature range from room temperature (RT) to 900 °C. Fig. 4 shows the dilatation (expansion) versus temperature curves for mullite, ZrO_2 and composites. All materials except MZ–15Y show a linear change in volume with temperature, suggesting that the phase transformation of ZrO_2 in these materials does not occur within this temperature range, the retained t-ZrO_2 phases in the zirconia polycrystals are metastable, and their phase transformation temperature is believed to be below RT.

In contrast, the MZ–15Y composite shows volume expansion and contraction with varying temperature which is accompanied by the tetragonal/monoclinic phase transformation. In other words, volume expansion occurs linearly with temperature during heating, until it contracts when the m-to-t phase transformation begins. Contraction continues to a temperature at which the phase transformation is complete (i.e. transformation proceeds over the temperature range), thereafter linear expansion is again found with temperature. On cooling, volume contraction and expansion resembling those on heating resulting from the t-to-m phase transformation, are observed. However, these two curves are not identical until they coincide at ambient temperature; as a result, a thermal hysteresis loop is established. The temperature for the start of the t-to-m phase transformation on cooling is expressed as M_s, in terms of the martensitic transformation. M_s for MZ–15Y was determined to be 613 °C by extrapolating the contraction and expansion curves. The dilatation curve of the MZ–15# material begins to alter near 900 °C on heating, which implies that the temperature for the m-to-t phase transformation is above 900 °C.

4. Conclusion

Mullite grains become smaller in composites on the addition of ZrO_2 particles (i.e. ZrO_2 particles retarded the grain growth of mullite). Relatively dense sintered body of mullite matrix/zirconia composite could be achieved by the use of yttria-stabilized zirconia and by employing the sol–gel prepared mullite/zirconia powder mixture. These two composites (MZ–15Y and MZ–15#) show fine microstructures and higher strengths. However, MZ–15M and MZ–15C are porous and their strengths degraded. The higher strength obtained in the sol–gel prepared mullite–ZrO_2 composite is, possibly, due to the free glass phase. ZrO_2 polycrystals consist predominantly of tetragonal phase; cubic phase incorporating t-ZrO_2 precipitates were contained in Mg–PSZ, but large fractions of ZrO_2 in the composites transformed to the monoclinic form. A sound composite body could not be attained by using 12Ce–TZP, which is attributed to the formation of deleterious internal voids. An expansion hysteresis effect was distinctly observed in the dilatation curve of MZ–15Y composite, in contrast to others, arising from the t–m phase transformation.

Acknowledgements

The authors thank Chichibu Onoda Cement Co. and Osaka Sumitomo Cement Co., for supplying the mullite and zirconia powders, respectively. The experimental assistance provided by H. Yamamoto, N. Mori, and R. Ozaki is also gratefully acknowledged.

References

1. F. J. KLUG, S. PROCHAZKA and R. H. DOREMUS, *J Amer. Ceram. Soc.* **70** (1987) 750.
2. H. SCHNEIDER and E. EBERHARD, *J. Amer. Ceram Soc.* **73** (1990) 2073.
3. B. B. GHATE, D. P. H. HASSELMAN and R. M. SPRIGGS, *Amer. Ceram. Soc. Bull.* **52** (1973) 670.
4. M. MIZUNO, *J. Amer. Ceram. Soc.* **74** (1991) 3017.
5. P. A. LESSING, R. S. GORDAN, and K. S. MAZDIYASNI, *ibid.* **58** (1975) 149.
6. B. L. METCALFE and J. H. SANT, *Trans. J. Br. Ceram. Soc.* **74** (1975) 193.
7. Y. OKAMOTO, H. FUKUDOME, K. HAYASHI and T. NISHIKAWA. *J. Eur. Ceram. Soc.* **6** (1990) 161.
8. M. D. SACKS and J. A. PASK, *J. Amer. Ceram. Soc.* **65** (1982) 65.
9. S. SOMIYA and Y. HIRATA, *Amer. Ceram. Soc. Bull.* **70** (1991) 1625.
10. M. G. M. U. ISMAIL, Z. NAKAI, and S. SOMIYA, *J. Amer. Ceram. Soc.* **70** (1987) C–7.
11. T. K. GUPTA, F. F. LANGE and J. H. BECHTOLD, *J. Mater. Sci.* **13** (1978) 1464.
12. T. K. GUPTA, J. H. BECHTOLD, R. C. KUZNICKI, L. H. CADOFF and B. R. ROSSING, *J. Mater. Sci.* **12** (1977) 2421.
13. R. C. GARVIE, R. H. HANNINK, R. T. PASCOE, *Nature* **258** (1975) 703.
14. D. L. PORTER and A. H. HEUER, *J. Amer. Ceram. Soc.* **60** (1977) 183.
15. J. S. MOYA and M. I. OSENDI, *J. Mater. Sci. Lett.* **2** (1983) 599.
16. N. CLAUSSEN and J. JAHN, *J. Amer. Ceram. Soc.* **63** (1980) 228.
17. P. BOCH, T. CHARTIER, and J. P. GIRY, in "Ceramic Transactions", Vol. 6, "Mullite and Mullite Matrix Composites", edited by S. Somiya, R. F. Davis, and J. A. Pask (American Ceramic Society, Westerville, OH, 1990) pp. 473–94.
18. R. TORRECILLAS, S. DE AZA, J. S. MOYA, T. EPICIER and G. FANTOZZI, *J. Mater. Sci. Lett.* **9** (1990) 1400.
19. H. G. SCOTT, *J. Mater. Sci.* **10** (1975) 1527.
20. C. T. GRAIN, *J. Amer. Ceram. Soc.* **50** (1967) 288.
21. P. DUWEZ and F. ODELL, *ibid.* **33** (1950) 274.

22. P. F. BECHER and M. V. SWAIN, *ibid.* **75** (1992) 493.
23. R. H. J. HANNINK and R. C. GARVIE, *J. Mater. Sci.* **17** (1982) 2637.
24. S. PROCHAZKA, J. S. WALLACE and N. CLAUSSEN, *J. Amer. Ceram. Soc.* **66** (1983) C125.
25. J. S. MOYA and M. I. OSENDI, *J. Mater. Sci.* **19** (1984) 2909.
26. G. ORANGE, G. FANTOZZI, F. CAMBIER, C. LEBLUD, M. R. ANSEAU and A. LERICHE *ibid.* **20** (1985) 2533.
27. H. SHIGA, M. G. M. U. ISMAIL and K. KITAYAMA, *J. Ceram. Soc. Jpn* **99** (1991) 798.
28. H. TORAYA, M. YOSHIMURA and S. SOMIYA, *J. Amer. Ceram. Soc.* **67** (1984) C119.
29. D. B. MARSHALL and A. G. EVANS, *ibid.* **64** (1981) C182.
30. F. F. LANGE, *J. Mater. Sci.* **17** (1982) 225.
31. A. G. EVANS and A. H. HEUER, *J. Amer. Ceram. Soc.* **63** (1980) 241.
32. T. MITSUHASHI, M. ICHIHARA and U. TATSUKE, *ibid.* **57** (1974) 97.
33. R. M. FULRATH, *ibid.* **42** (1959) 423.
34. K. B. ALEXANDER, P. F. BECHER, X. L. WANG and C. H. HSUEH, *ibid.* **78** (1995) 291.
35. T. M. KYAW, Y. OKAMOTO and K. HAYASHI, *J. Jpn Soc. Powder Powder Metall.* **42** (1995) 918.
36. T. MASAKI, *J. Amer. Ceram. Soc.* **69** (1986) 638.
37. M. RUHLE and A. H. HEUER, in "Advances in Ceramics", Vol. 12, "Science and Technology of Zirconia II", edited by N. Claussen, M. Ruhle and A. H. Heuer (American Ceramic Society, Columbus, OH 1984) p. 14.
38. T. K. GUPTA, *J. Amer. Ceram. Soc.* **63** (1980) 117.
39. M. V. SWAIN, *J. Mater. Sci.* **15** (1980) 1577.
40. D. J. GREEN, *J. Amer. Ceram. Soc.* **66** (1983) 807.
41. R. J. PANLENER and R. N. BLUMENTHAL, in "Phase Diagrams for Ceramists", Vol. 4, edited by R. S. Roth, T. Negas and L. P. Cook (American Ceramic Society, Westerville, OH, 1981) p. 228.
42. T. NEGAS, R. S. ROTH, C. L. McDANIEL, H. S. PARKER and C. D. OLSON, *ibid*, *p.* 228.
43. E. TANI, M. YOSHIMURA and S. SOMIYA, *J. Amer. Ceram. Soc.* **66** (1983) 506.
44. P. DURAN, M. GONZALEZ, C. MOURE, J. R. JURADO and C. PASCUAL, *J. Mater*, *Sci.* **25** (1990) 5001.
45. K. H. HEUSSNER and N. CLAUSSEN, *J. Amer. Ceram. Soc.* **72** (1989) 1044.
46. A. A. TOROPOV, I. F. ANDREEV, A. N. SOKOLOV and L. N. SANZHAREVSKAYA, in "Phase Diagrams for Ceramists", Vol. 4, edited by R. S. Roth, T. Nagas and L. P. Cook (American Ceramic Society, Westerville, OH, 1981) p. 229.
47. V. LONGO and L. PODDA, *ibid*., p. 228.
48. A. I. LEONOV, A. V. ANDREEVA, V. E. S. SHVAIKOVSKII and E. K. KELER, in "Phase Diagrams for Ceramists", 1975 Supplement, edited by E. M. Levin and H. F. McMurdie (American Ceramic Society, Westerville, OH, 1975) p. 130.
49. K. ANDO, S. MORITA and R. WATANABE, *Yogyo Kyokaishi* **94** (1986) 732.

Received 20 November 1995
and accepted 4 April 1997